Iranian Journal of Electrical and Electronic Engineering 03 (2020) 412–424
Special Issue on Smart Grids

Iranian Journal of Electrical and Electronic Engineering

Journal Homepage: ijeee.iust.ac.ir

Research Paper

Very Fast Load Flow Calculation Using Fast-Decoupled Reactive Power Compensation Method for Radial Active Distribution Networks in Smart Grid Environment Based on Zooming Algorithm

O. Honarfar* and A. Karimi*(C.A.)

Abstract: Distribution load flow (DLF) calculation is one of the most important tools in distribution networks. DLF tools must be able to perform fast calculations in real-time studies at the presence of distributed generators (DGs) in a smart grid environment even in conditions of change in the network topology. In this paper, a new method for DLF in radial active distribution networks is proposed. The method performs a very fast DLF using zooming algorithm associated with a fast-decoupled reactive power compensation (ZAFDRC) technique, not in all of the buses of the grid, causes to reduce the solution time, which is the most important issue in the real-time studies. The proposed method is based on the zooming algorithm and does not require to calculate the bus-injection to branch-current (BIBC) matrix which reduces the computational burden and helps to decrease the solution time. The method is tested on the IEEE 69-bus systems as a balanced network and the IEEE 123-bus as a very unbalanced system. The results confirm the high accuracy and high speed of the proposed method.

Keywords: Active Distribution Networks, Distribution Load Flow (DLF), Radial Systems, Smart Grid, Zooming Algorithm.

1 Introduction

IN recent years, using of DGs in medium and low voltage distribution networks has been significantly increased. These resources are used to solve problems with the distribution network by reducing losses, supporting voltage, providing backup power and ancillary services, improving reliability, and deferring network upgrade [1]. Because of integration of smart metering devices, distributed energy storage units, and distributed generation (DG) plants, the structure of the modern power grids is suffering important changes [2]. Actually, the distribution network is passing through a passive to an active and an intelligent structure. This makes it possible to use distributed energy resources [3, 4]. Many of the functions used in the smart distribution system need a simple and fast way of computing the load flow solution [5]. The load flow problem is one of the main tasks in power system applications. Actually, it expresses the link between complex node voltages and complex nodal power injections [6]. DLFs are needed for analyzing the voltage profile, power flows, and losses, to determine the basic capacity and voltage regulation issues associated with DG interconnection [7]. In real-time studies, a very fast DLF method, which its results can be employed quickly by the control system, is highly needed. The issue of the load flow solution time is a controversial and disputed subject within the field of the smart grids DLFs. An extended distribution system and its inherent imbalances increase the size of the DLFs and the solution time and make the performance of the control system ineffective [8].

The classical ways of the DLF are divided into two

Iranian Journal of Electrical and Electronic Engineering, 2020.
Paper first received 15 February 2019, revised 25 September 2019, and accepted 06 October 2019.
* The authors are with the Faculty of Electrical and Computer Engineering, University of Kashan, Kashan, Iran.
E-mails: omid.honarfar@grad.kashanu.ac.ir and a.karimi@kashanu.ac.ir.
Corresponding Author: A. Karimi.

categories, methods based on Newton-Raphson (NR) and methods based on backward/forward sweep (BFS). The NR method almost shows constant iterations in large-scale and balanced systems [9]. Because of the convergence problems associated with the radial topology and high R/X (resistance to reactance) ratio of the distribution network systems and the large memory requirement for the computer storage, the NR based methods are not proper to be employed in such networks [10, 11]. Though, the BFS based methods can be easily used in the radial distribution networks. The problem associated with such methods is that the solution time of this kind of methods is considerably depended on the size of the system and it is significantly increased in the real networks with thousand buses. The ladder-network theory has been proposed in [12] to cope with the radial distribution networks. This method performs several BFSs in each iteration. The graph theory-based radial load flow analysis is proposed in [13], which helps in arranging line data connections for any tie switch position combinations. In [14] the interior based power flow solution is proposed for balanced microgrid operating in islanding mode. The proposed method can consider voltage-dependent and frequency-dependent loads and has a good convergence ability. The decomposed quasi-Newton method for unbalanced networks is proposed in [15]. The method has robust convergence ability and high performance for distribution networks when ill-conditioned. The agent-based decentralized DLF for weakly meshed distribution systems is proposed in [16]. The proposed method is fast and efficient compared with centralized approach. In [17] a novel algorithm using an improved evolutionary algorithm is proposed which solves the power flow in islanding microgrids without considering the slack bus. In [18] a generalized Hopfield neural network is proposed to solve the non-linear load flow equations. The method is simple to use and has faster convergence and less calculation burden compared with the NR method. In [19], the recursive power flow algorithm is proposed to overcome the drawbacks of the distribution load flow method to consider the detailed model of transformers. This method has no significant computational burden difference compared with conventional methods. A fast and efficient DLF based on the BFS method is proposed in [20]. This method performs the very fast DLF and it is suitable to be used in passive networks with no DG units. In [21], the DLF method has been proposed that converts a PQ load to its equivalent impedance and solves the problem. This method cannot be used in cases including the PV buses. In [22], the Z-bus based Gauss iterative method presented in [23] is implemented for radial networks having the PQ buses. The quadratic based method is proposed in [24]. In this method, both voltage magnitude and phase angle are computed simultaneously. An adaptive technique based on BFS for distribution systems with PV buses is proposed in [25]. In this paper, the injected current by the PV bus is updated when the voltage of the PV bus exceeds the limits. In [26] and [27], a BFS based method is proposed that includes matrix inversion. Using such an approach in online studies imposes a great calculation burden on the computer and makes the solution time very long. In [28], a DLF approach using a zooming algorithm is developed. This algorithm solves the load flow problem in a specific area of interest in the distribution system without requiring the presence of all of the system buses. The area of interest is established based on a user-input bus, called zoom-in bus. The method presented in [28] is useful for DLF in the networks with the radial structure that there is no DG operating in PV-mode.

The special objective of this paper is describing the zooming algorithm proposed in [28], DG modeling declared in [29] (which is called decoupled reactive compensation method here) and proposing a novel algorithm used for DLF at the presence of DGs operating in PV-mode using the proposed fast-decoupled reactive compensation method (FDRC) in radial distribution networks where the real-time studies are highly needed like the smart distribution networks. This technique solves the DLF problem using BFS at the presence of DG units operating in PV-mode causes the solution time to be declined very much. Table 1 shows the features of the proposed method compared to [28] and [29]. In summary, the main contributions of this paper are as follows:

- The fast-decoupled reactive compensation (FDRC) method is proposed, associated with the zooming algorithm (ZAFDRC) and used for the DLF issue which significantly helps to improve the solution time. The method is appropriate for the networks having DGs working in PV-mode. The comparison of the results of the proposed method with the traditional BFS method under the same condition validates the high accuracy and the high speed of the

Table 1 Features of the proposed method compared to [28] and [29].

Features	[28]	[29]	Proposed method
Network topology	Radial	Radial	Radial
System condition	Balanced and unbalanced	Balanced and unbalanced	Balanced and unbalanced
DG	Yes	Yes	Yes
PV bus	–	Yes	Yes
Basic calculation	BFS method	BFS method	BFS method
Network modeling way	Defining physical connection matrix using bus-injection to branch-current matrix	KCL and KVL approaches	Defining physical connection matrix using Ybus matrix
Reduction of network size	Lumping technique	–	Lumping technique

proposed method.

- A new physical connection (PC) matrix building method is proposed which makes it more flexible to build the PC matrix and also causes its building time to be reduced.

The rest of this paper is organized as follows. Section 2, allots to the model description. In Subsection 2.1, the lumping technique is explained which helps to size reduction of the system. Subsection 2.2 discuses about DG modeling in the PV-mode. In this section, the FDRC approach is also proposed. The way of the network modeling is explained in Subsection 2.3. A new algorithm for building the PC matrix is proposed in Section 3. Section 4 discusses the zooming algorithm at the presence of DGs. Section 5 consists of the simulation results. In this section, DLF is performed using the zooming algorithm method associated with the FDRC approach (ZAFDRC). The simulation is performed using the IEEE 69-bus system as a balanced network and the IEEE 123-bus system as a very unbalanced with low convergence ability distribution network. Finally, the conclusion is presented in Section 6.

2 Model Description

This section describes the way of modeling of different parts of the distribution network.

2.1 Lumping Technique

One of the most important ways of decreasing the load flow solution time in BFS based methods is decreasing the size of the network. The lumping technique proposed in [28] reduces the size of the network by replacing some of the feeders by their equivalent PQ load. This is done by dividing feeders of the network into two categories, main feeders, and lateral feeders. The main ones include those feeders that are considered in the zooming based DLF for specific objectives like determining the set point of the DG units. The lateral feeders include those feeders that are replaced by their equivalent PQ load. The power injected in any lateral feeder is divided into two components: the total connected load and the active and the reactive power losses of each feeder. The lumping technic makes it possible to calculate the total power supplied to the feeder approximately. As an example, assume the single-phase feeder *f* shown in Fig. 1. This feeder contains many sections. The total active and reactive power supplied by this feeder (S_f) can be calculated by (1) as follows:

$$S_f = \left(\sum P_{Load_f} + \sum_s P_{Loss_{f_s}} \right) + j \left(\sum Q_{Load_f} + \sum_s Q_{Loss_{f_s}} \right) \quad (1)$$

where $\sum P_{Load_f}$ and $\sum Q_{Load_f}$ represent the total active and reactive load connected to the feeder *f*. $\sum P_{Loss_{f_s}}$ and $\sum Q_{Loss_{f_s}}$ show the sum of the active and reactive power losses of each section of the feeder, respectively. $P_{Loss_{f_s}}$ and $Q_{Loss_{f_s}}$ represent the active and reactive power losses of each section of the feeder and can be calculated using (2) and (3) as follows:

$$P_{Loss_{f_s}} = \frac{P_{Load_s}^2 + Q_{Load_s}^2}{V_s^2} R_s \quad (2)$$

$$Q_{Loss_{f_s}} = \frac{P_{Load_s}^2 + Q_{Load_s}^2}{V_s^2} X_s \quad (3)$$

where V_s is the magnitude of the voltage at the receiving bus in section *s*. In the first time, V_s is assumed to be equal to the nominal voltage. R_S, X_S show the resistance and reactance of section s, respectively. P_{Load_s} and Q_{Load_s} represent the active and reactive power flowing through each section, respectively.

2.2 DG Modeling

DGs can be considered as a constant power factor generator (the PQ bus) or as a voltage-controlled generator (the PV bus). Generally, a DG unit is working in the PQ mode, where the power injected to the network by a generator is considered as a negative load, while in PV-mode, a mathematical model is needed to compute the reactive power supplied by the generator. This model can be achieved by the compensation method. Using the compensation method, the impedance matrix of the Thevenin equivalent circuit of DGs can be calculated. According to [29], the relation of voltages and currents in the p.u. system at the DG connection bus is calculated as follows:

$$\mathbf{Z}\bar{\mathbf{I}} = \bar{\mathbf{V}} \quad (4)$$

where $\bar{\mathbf{V}}$ and $\bar{\mathbf{I}}$ are the voltage and current vectors of DG units, respectively. Equation (4) can be modified as (5).

$$\mathbf{Z}\Delta\bar{\mathbf{I}} = \Delta\bar{\mathbf{V}} \quad (5)$$

Regarding that the network voltage is near the nominal voltage and the voltage angle is small we will have:

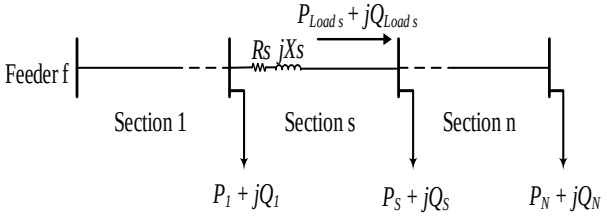

Fig. 1 Single-phase feeder.

$$\Delta\bar{\mathbf{S}}^{*} = \Delta\bar{\mathbf{V}}^{*} \times \Delta\bar{\mathbf{I}} \quad \rightarrow \quad \Delta\bar{\mathbf{S}}^{*} \cong \Delta\bar{\mathbf{I}} \tag{6}$$

With replacement (6) in (5) we have:

$$\mathbf{Z}\Delta\bar{\mathbf{S}}^{*} = \Delta\bar{\mathbf{V}} \tag{7}$$

In the complex plane, (11) is shown as follows:

$$\mathbf{Z} = \mathbf{R} + j\mathbf{X} \tag{8}$$

$$\Delta\bar{\mathbf{S}}^{*} = \Delta\bar{\mathbf{P}} - j\,\Delta\bar{\mathbf{Q}} \tag{9}$$

$$\bar{\mathbf{V}} = \Delta\bar{\mathbf{V}} + j\,\Delta\bar{\boldsymbol{\delta}} \tag{10}$$

which is culminated in (11).

$$\left(\mathbf{R} + j\mathbf{X}\right) \times \left(\Delta\bar{\mathbf{P}} - j\,\Delta\bar{\mathbf{Q}}\right) = \left(\Delta\bar{\mathbf{V}} + j\,\Delta\bar{\boldsymbol{\delta}}\right) \tag{11}$$

Equation (11) can be written as (12) and (13).

$$\mathbf{R}\Delta\bar{\mathbf{P}} + \mathbf{X}\Delta\bar{\mathbf{Q}} = \Delta\bar{\mathbf{V}} \tag{12}$$

$$\mathbf{X}\Delta\bar{\mathbf{P}} - \mathbf{R}\Delta\bar{\mathbf{Q}} = \Delta\bar{\boldsymbol{\delta}} \tag{13}$$

Above equations can be written in matrix form as follow:

$$\begin{bmatrix} \mathbf{X} & \mathbf{R} \\ -\mathbf{R} & \mathbf{X} \end{bmatrix} \begin{bmatrix} \Delta\bar{\mathbf{Q}} \\ \Delta\bar{\mathbf{P}} \end{bmatrix} = \begin{bmatrix} \Delta\bar{\mathbf{V}} \\ \Delta\bar{\boldsymbol{\delta}} \end{bmatrix} \tag{14}$$

Due to that DG is working in the PV-mode, (14) can be rewritten as follow:

$$\left[\mathbf{X}\right]\left[\Delta\bar{\mathbf{Q}}\right] = \left[\Delta\bar{\mathbf{V}}\right] \tag{15}$$

Here, (15) is defined as the decoupled reactive compensation equation used to model DG units working in the PV-mode and determines the reactive power injected by the DGs. In (15), **X** is called the sensitivity matrix and contains only the reactance of the lines. The dimension of this matrix equals to $m \times m$, where m is the number of DGs working in PV-mode. As it was shown before, (15) is achieved after many simplifications and also, the effect of voltage angle and the line resistance are neglected. This simplification helps to reduce the calculation burden on the computer and causes the convergence speed reduction for calculating (or compensating) $\Delta\bar{\mathbf{Q}}$ according to (15). The convergence speed reduction causes the BFS iterations to be increased and makes the solution time longer. To overcome this problem, using (15), the fast-decoupled reactive compensation method is proposed here as follows:

$$\left[\bar{\mathbf{X}}\right]\left[\Delta\bar{\mathbf{Q}}\right] = \alpha\left[\Delta\bar{\mathbf{V}}\right] \tag{16}$$

Here a factor named compensation factor is added to (15). The compensation factor α, is a real number that improves the convergence speed reduction caused during the simplifications. This compensation factor also causes the BFS iterations to be decreased during the DLF at the DG presence and so the solution time will be decreased subsequently. Since α is a single number, it does not increase the matrix dimension so the calculation burden is not increased very much. The compensation factor can be tuned well using the intelligent algorithms or the way of trial and error, for every network. Since the network topology is not changed quickly, this factor should not be tuned every time. The way of building of the matrix **X** is shown according to Fig. 2. The diagonal elements of the matrix are equal to the summation of the reactance of the lines, which are located between every DG and the slack bus. Other elements consist of summation of the reactance of the lines that are common in the path between DG and the slack bus for two DGs. According to this, we will have:

$$\mathbf{X} = \begin{bmatrix} 0.8 & 0.3 \\ 0.3 & 1 \end{bmatrix} \tag{17}$$

Using the above concept, the sensitivity matrix **X** can be extended to include the mutual inductance. In this case, **X** includes the mutual inductance, too. According to this, we will have:

$$\mathbf{X}_{q} = \begin{bmatrix} \mathbf{X}^{g_1 t} & \mathbf{X}^{(g_1+g_2)t} \\ \mathbf{X}^{(g_1+g_2)t} & \mathbf{X}^{g_2 t} \end{bmatrix} \tag{18}$$

where $\mathbf{X}_q$, is the sensitivity matrix in the positive sequence and $\mathbf{X}^{g_1 t}$ is calculated as follows:

$$\mathbf{X}^{g_1 t} = \begin{bmatrix} \mathbf{X}_{aa}^{g_1} & \mathbf{X}_{ab}^{g_1} & \mathbf{X}_{ac}^{g_1} \\ \mathbf{X}_{ab}^{g_1} & \mathbf{X}_{bb}^{g_1} & \mathbf{X}_{bc}^{g_1} \\ \mathbf{X}_{ac}^{g_1} & \mathbf{X}_{bc}^{g_1} & \mathbf{X}_{cc}^{g_1} \end{bmatrix} \tag{19}$$

where $\mathbf{X}_{aa}^{g_1}$, $\mathbf{X}_{bb}^{g_1}$, $\mathbf{X}_{cc}^{g_1}$ show the self-inductance and $\mathbf{X}_{ab}^{g_1}$,

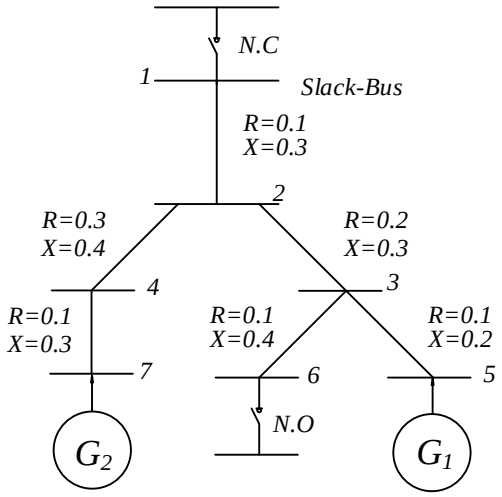

Fig. 2 Sample 7-bus system used for sensitivity matrix calculation.

$\mathbf{X}_{bc}^{g_1}$, $\mathbf{X}_{ca}^{g_1}$ show the mutual inductance of the 3-phase branches located between DG1 and the slack bus. Matrix $\mathbf{X}^{g_2 t}$ is also derived like $\mathbf{X}^{g_1 t}$ for DG2. $\mathbf{X}^{(g_1+g_2)t}$ consists of the summation of line inductance which are common in the path between DG and the slack bus for DG1 and DG2. Here, during calculating the DLF, the convergence criterion is defined using both voltage error and calculated reactive power. The reactive power injected by the DG can be calculated as follows:

1. First, after the DLF is calculated, ΔV_1^i is computed by (20) and then it is checked to be less than a specified value as follows:

$$\Delta V_1^i = \left|V_{1spec}^i\right| - \left|V_{1cal}^i\right| \qquad i \in \{PV\ nodes\} \tag{20}$$

where ΔV_1^i shows the voltage error in positive sequence, ΔV_{1spec}^i shows the reference voltage in the positive sequence, and ΔV_{1cal}^i is the calculated voltage in node *i*.

2. If ΔV_1^i is less than a specified value ($\Delta V_1^i \le \beta$) then the voltage of node i is converged and the DLF solution finishes. Otherwise, reactive power (ΔQ) must be calculated using (21). If $\Delta V_1^i > \beta$, then the injected reactive power must be decreased by ΔQ. If $\Delta V_1^i < -\beta$, then the injected reactive power must be increased by ΔQ. So, the new value of the reactive power, Q^i_{new}, is calculated as below:

$$Q_{new}^i = Q_{old}^i \pm 3\times\left|\Delta Q^i\right| \tag{21}$$

3. Now the calculated reactive power is set to the DG as follows and DLF runs again:

$$\begin{cases} If\ \ Q_{G,\min}^i < Q_{new}^i < Q_{G,\max}^i \Rightarrow Q_G^i = Q_{new}^i \\ If\ \ Q_{new}^i < Q_{G,\min}^i \Rightarrow Q_G^i = Q_{G,\min}^i \\ If\ \ Q_{G,\max}^i < Q_{new}^i \Rightarrow Q_G^i = Q_{G,\max}^i \end{cases}$$

where $Q_{G,\max}^i$ and $Q_{G,\min}^i$ represent the maximum and minimum reactive power generated by DG respectively and Q^i_G represents the reference value of reactive power [29]- [30]. This process is repeated until the convergence criterion is reached.

2.3 Network Modeling

Typically, the short line equivalent circuit is used to model the network in distribution systems (for example, the IEEE 69-bus system). Nonetheless in some distribution networks such as the IEEE 123-bus system (a feeder with a 4.16kV operating voltage, overhead and underground lines, shunt capacitors, and unbalanced loading), the capacitance of the lines is not negligible, so the equivalent π circuit is used to model this network. The equivalent π circuit and the short line equivalent circuit are shown in Figs. 3(a) and (b), respectively. To calculate the voltage of the sending bus in the equivalent π circuit, I_A, I_B, and I_C are calculated as follows:

$$I_A = \left(\frac{P_A + jQ_A}{V_{AB}}\right)^* - \left(\frac{P_C + jQ_C}{V_{CA}}\right)^* + j\,\omega\left(C_{AB}\times V_{AB} - C_{CA}\times V_{CA}\right) \tag{22}$$

$$I_B = \left(\frac{P_B + jQ_B}{V_{BC}}\right)^* - \left(\frac{P_A + jQ_A}{V_{AB}}\right)^* + j\,\omega\left(C_{BC}\times V_{BC} - C_{AB}\times V_{AB}\right) \tag{23}$$

$$I_C = \left(\frac{P_C + jQ_C}{V_{CA}}\right)^* - \left(\frac{P_B + jQ_B}{V_{BC}}\right)^* + j\,\omega\left(C_{CA}\times V_{CA} - C_{BC}\times V_{BC}\right) \tag{24}$$

Now the voltage of the sending bus can be calculated as follows:

$$V_{AB\,S} = V_{AB} + Z_A\times I_A + Z_{AB}\times I_B + Z_{CA}\times I_C - (Z_B\times I_B + Z_{AB}\times I_A + Z_{BC}\times I_C) \tag{25}$$

$$V_{BC\,S} = V_{BC} + Z_B\times I_B + Z_{AB}\times I_A + Z_{BC}\times I_C - (Z_C\times I_C + Z_{CA}\times I_A + Z_{BC}\times I_B) \tag{26}$$

$$V_{CA\,S} = V_{CA} + Z_C\times I_C + Z_{CA}\times I_A + Z_{BC}\times I_B - (Z_B\times I_B + Z_{AB}\times I_A + Z_{BC}\times I_C) \tag{27}$$

To calculate the network voltage, the mutual impedances have been considered. Active and reactive power losses are calculated as below:

$$P_{loss} + jQ_{loss} = P_{tot} + jQ_{tot} - \left(\sum P_{Load} + j\sum Q_{Load}\right) \tag{28}$$

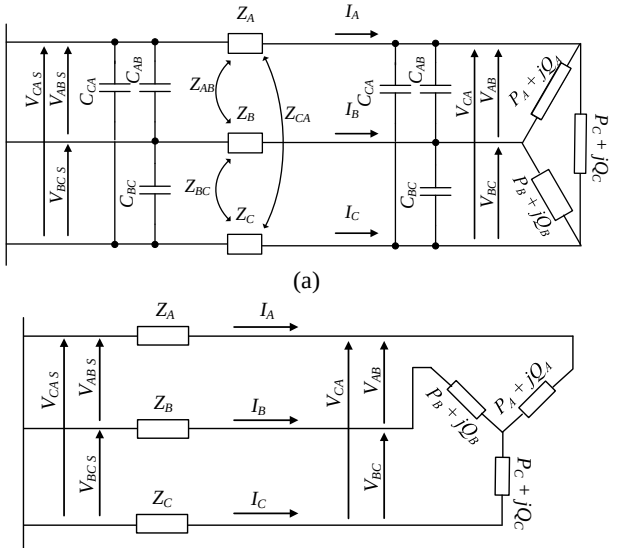

Fig. 3 a) The equivalent π circuit and b) The short line equivalent circuit.

where P_{tot} and Q_{tot} represent the total active and reactive power supplied by the slack bus, respectively. ΣP_{Load} + $j\Sigma Q_{Load}$ represents the total connected load to the network. P_{tot} + jQ_{tot} is calculated as follows:

$$P_{tot} + jQ_{tot} = V_{AB} \times (I_A)^* + V_{BC} \times (I_B)^* + V_{CA} \times (I_C)^* \quad (29)$$

The short line equivalent circuit (in this paper, the IEEE 69-bus system) is modeled according to Fig. 3(a). Therefore, the line currents are calculated as follows:

$$I_A = \left((P_A + jQ_A) \Big/ \frac{V_{AB}}{\sqrt{3}\angle 30} \right)^* \quad (30)$$

$$I_B = \left((P_B + jQ_B) \Big/ \frac{V_{BC}}{\sqrt{3}\angle 30} \right)^* \quad (31)$$

$$I_C = \left((P_C + jQ_C) \Big/ \frac{V_{CA}}{\sqrt{3}\angle 30} \right)^* \quad (32)$$

Now the voltage of the sending bus can be calculated as below:

$$V_{ABS} = V_{AB} + Z_A \times I_A - Z_B \times I_B \quad (33)$$

$$V_{BCS} = V_{BC} + Z_B \times I_B - Z_C \times I_C \quad (34)$$

$$V_{CAS} = V_{CA} + Z_C \times I_C - Z_A \times I_A \quad (35)$$

The active and reactive power losses can be calculated using (28) and (29).

3 New Method of PC Matrix Building

The distribution network connections are modeled using the PC matrix as mentioned in [28]. The PC matrix is a matrix that defines the connections among the system buses. The PC matrix of the sample 7-bus system supplied by bus 1 is shown as follows.

Upstream buses

	1	2	3	4	5	6	7	
	1	1	1	1	1	1	1	1
	0	1	1	1	1	1	1	2
$PC =$	0	0	1	0	1	1	0	3
	0	0	0	1	0	0	1	4
	0	0	0	0	1	0	0	5
	0	0	0	0	0	1	0	6
	0	0	0	0	0	0	1	7

Downstream buses

A new procedure of building the PC matrix is proposed here to reduce the matrix building time. To decrease the computational burden and the DLF solution time, $\mathbf{Y}_{BUS}$ or $\mathbf{Z}_{BUS}$ matrix of the system are proposed here to be used instead of the bus-injection to branch-current (BIBC) matrix as mentioned in [28], which imposes additional data during the PC matrix building. Here, only the radial systems are considered. For all buses except the slack bus, two groups of buses are defined as upstream and downstream buses. All the buses supplied through a specific bus are called downstream buses of that bus (corresponding to the horizontal direction of PC matrix), and the buses which play supplying role for a specific bus are called upstream buses of that bus (corresponding to the vertical direction of PC matrix). In other words, for a specific bus, upstream buses consist of buses that connect that bus to the slack bus and the downstream ones consist of buses that are supplied by the bus. This concept helps us to build the PC matrix of the network only if we know the slack bus and the $\mathbf{Y}_{BUS}$ or $\mathbf{Z}_{BUS}$ matrix of the network, so the PC matrix can be created without using the BIBC matrix. Also, the slack bus of the system can be changed if the network is supplied by more than one slack bus for emergency conditions. So, the PC matrix can be easily updated and changed in every time needed only by changing the slack bus while the BIBC matrix must be defined again according to the new structure. The flowchart of the proposed PC matrix building algorithm is shown in Fig. 4. For example, the calculated PC matrix in the sample 7-bus system shown in Fig. 2 is for the case that bus 1 is determined as the slack bus. Now suppose that there is another bus connected to bus 6 by a tie line and the distribution network can be supplied by that bus too. If bus 6 supplies the network, this bus is considered as the slack bus. Now to calculate the load flow, first, we need to build the PC matrix corresponding to the new structure. In this way, the BIBC matrix corresponding to the new structure must be defined again while $\mathbf{Y}_{BUS}$ or $\mathbf{Z}_{BUS}$ matrix of the system is as before yet and can be easily used to build the PC matrix according to the concept declared above. The PC matrix of the new structure (supplied by bus 6) has been shown as follows.

Upstream buses

	6	3	2	5	1	4	7	
	1	1	1	1	1	1	1	6
	0	1	1	1	1	1	1	3
$PC =$	0	0	1	0	1	1	1	2
	0	0	0	1	0	0	0	5
	0	0	0	0	1	0	0	1
	0	0	0	0	0	1	1	4
	0	0	0	0	0	0	1	7

Downstream buses

In this paper, the way of the PC matrix building is described based on $\mathbf{Y}_{BUS}$ matrix. The detailed algorithm is described as following:

1. $\mathbf{Y}_{BUS}$ or $\mathbf{Z}_{BUS}$ matrix of the network is read and a zero matrix with a dimension as the same of the $\mathbf{Y}_{BUS}$ or $\mathbf{Z}_{BUS}$ matrix is created.
2. Slack bus is determined and chosen as the first

member of the PC matrix.

3. New members of the PC matrix are defined as the upstream buses and the corresponding rows and columns are changed to 1.
4. The downstream bus(es) that is/are directly connected to the upstream bus(es) is/are defined through the $\mathbf{Y}_{BUS}$ or $\mathbf{Z}_{BUS}$ matrix and if existing, repetitive bus(es) is/are removed. Regarding the remaining ones and the upstream bus(es), the rows and columns are changed to 1 in the PC matrix.
5. If the dimension of the PC matrix is not equal to the dimension of $\mathbf{Y}_{BUS}$ or $\mathbf{Z}_{BUS}$ matrix go to step 3.
6. Show the PC matrix.

In this way, any change in the structure of the network can be considered, so the new PC matrix of the system can be calculated according to the new structure. To show the effect of eliminating the BIBC matrix, a comparison between the PC matrix building time of the method used in [28] and the proposed method is done and the results are shown in Table 2. The laptop hardware characteristics are also shown in Table 2. The flowchart of the proposed PC matrix building method is shown in Fig. 4.

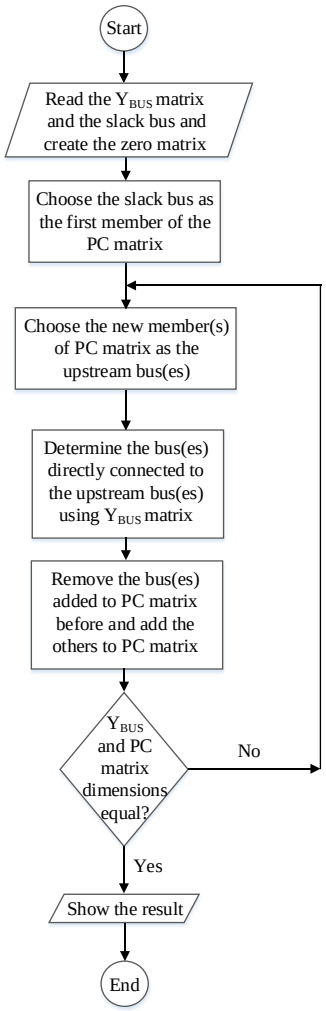

Fig. 4 Flowchart of the PC matrix building procedure.

4 Zooming Algorithm at Presence of DG Units Operating in PV-Mode

In Fig. 5, the flowchart of the proposed algorithm at the presence of DGs is illustrated. The algorithm starts by building the PC matrix. After that, the zoom-in bus (here called destination bus), the bus which determines a path from the slack bus to calculate the load flow, is determined according to the requirements of the dispatching center, and then the network information is updated. This information consists of DG capacities and load data. After identifying the buses which the lumping technique must be performed on them and after calculating their equivalent PQ load, the DLF begins according to the PC matrix. When the voltage convergence is achieved, DGs working in the PV-mode are considered to work at the specified voltage. If the specified voltage is not achieved, the amount of the injected reactive power is changed according to the desired voltage and the DLF runs again until the voltage convergence is achieved and the specified voltage (as the convergence criteria) is reached.

Table 2 Comparison of the time required to build the PC matrix of the IEEE 123 bus system.

Method	Time [ms]	The laptop characteristics
Method used in [28]	72.9	Intel® Core i5 Processor with 4 GB RAM
Proposed method	52.2	Intel® Core i5 Processor with 4 GB RAM
	11.9	Intel® Core i7 Processor with 8GB RAM

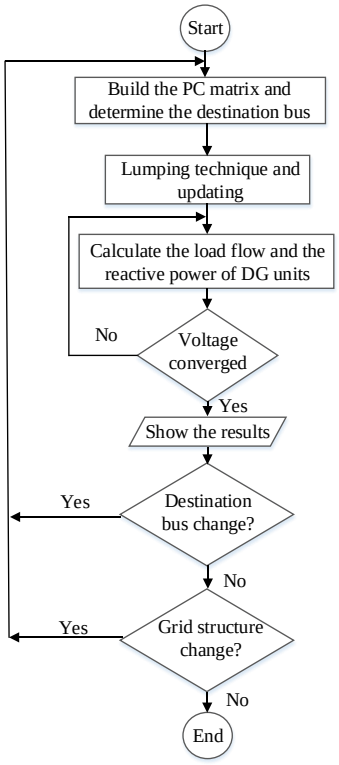

Fig. 5 Flowchart of the proposed algorithm at the presence of DGs.

5 Simulation Results

In this section, the DLF of the IEEE 69-bus (as a balanced radial network) and the IEEE 123-bus (as an unbalanced and radial network) systems at the presence of DG units is obtained at different cases and the results are compared to verify the speed and accuracy of the proposed method.

5.1 IEEE 69-Bus System

In this case, it is supposed that three DG units are located at buses 17, 50, 61 on the IEEE 69-bus system and the load flow is calculated on the sections shown in Fig. 6. The black solid path in Fig. 6 shows the case, that there are three DGs connected to the network. The grey paths present the lateral feeders and dot-dashed and dashed paths show the cases that there are 2 and 1 DG(s) connected to the network respectively. In this case, DGs are modeled as PV buses as declared in Section 2.

Using (16) rather than (15) causes the convergence to be achieved more quickly and hence the solution time will be decreased. To show this, first, the load flow is calculated by α = 1 (Eq. (15)) and after that, α is supposed to be equal to 7000 (the proposed method). The capacity of DGs and the buses that those are connected to are chosen based on the data presented in [31]. These data are shown in Table 3.

First of all, in each case, the load flow of the network according to the data presented in Table 3 is calculated and the voltage of the buses having the DG is obtained and chosen as V_{1spec}^{i}. Here a scenario is considered. In this scenario, it is assumed that the total injected reactive power by the DGs (referred to the data in Table 3) is decreased by 150kVAr. This reactive power reduction is proportional to each DG capacity in each case and the new injected reactive power is chosen as predefined reactive power. In this way, the network voltages become different from the base case (when there is no reactive power reduction). Under this condition, the load flow is run and the reactive power of the DGs starts to be calculated (increase until the reduced reactive power is compensated) until the V_{1spec}^{i} is achieved.

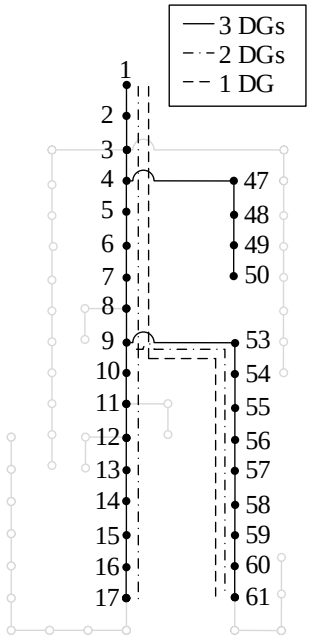

Fig. 6 Single line diagram of the IEEE 69-bus system.

For example, assume the case with one DG unit in Table 4. It is injecting 1283.81kVAr (desired reactive power in Table 4) to the network. Under this condition, the voltage of bus 61 is equal to 0.9998p.u. This voltage is chosen as V_{1spec}^{61}. Now the injected Q is reduced up to 150kVAr (Q = 1133.81) and so the voltage of bus 61 decreases too. After that, the DLF is run to calculate the reactive power (calculated reactive power in Table 4) which makes the voltage of bus 61 equal to 0.9998. In order to show the effect of α, the load flow in each case is calculated using α = 1 and α = 7000 (chosen by trial and error). The DLF time is computed in each case and the results are shown in Table 4. As the simulation results show, the solution time with α = 7000 (the proposed method) is decreased very much in comparison with α = 1. For a better comparison, in the first case, the solution time of the DLF of the whole of the grid is presented. In this case, the zooming algorithm is not used (the whole of the grid is studied) and DG resources are not considered (it is assumed that there are no DG resources connected). Comparing the first case with the other cases (where the zooming algorithm is used and DG resources working in PV-mode are connected) in table 4 and 8 where α = 1, shows that, zooming algorithm won't have an effective performance when PV-buses are included. This shows that the zooming algorithm has a high performance if the buses of the network are modeled as PQ-buses and it does not work properly at the presence of PV modeled buses.

As it is seen from Table 4, when the load flow is calculated using ZAFDRC, as the number of the

Table 3 Data of DGs connected to the IEEE 69-bus system.

Cases	Installed DG schedule			
1 DG connected	Bus	61		
	Size [kVA]	2250		
	P DG [kW]	1839.26		
	Q DG [kVAr]	1283.81		
	voltage @ bus [p.u.]	0.9998		
2 DGs connected	Bus	61	17	
	Size [kVA]	2250	670	
	P DG [kW]	1799.9	540.38	
	Q DG [kVAr]	1256.34	377.19	
	voltage @ bus [p.u.]	1.0024	1.0012	
3 DGs connected	Bus	61	17	50
	Size [kVA]	2250	670	850
	P DG [kW]	1699.86	510.04	679.78
	Q DG [kVAr]	1186.51	356.01	474.49
	voltage @ bus [p.u.]	0.9979	0.9989	0.9996

connected DG units to the grid increases, the DLF time increases too. This is because of the size increment of the sensitivity matrix and the more buses that must be considered during the DLF which increases the size of the problem. For a better comparison between the traditional BFS load flow and the proposed method, the DLF time of the whole of the grid with no DG unit (as the fastest DLF with no DG unit operating in PV-mode) is also presented in Table 4. Comparing the case with no DG unit with the other cases shows that the proposed method works much faster than the traditional BFS method when there is no DG unit connected to the network and the distribution system is modeled only by PQ buses. The data presented in Table 4 and different comparisons validate the high speed of the proposed method.

The calculated voltages by ZAFDRC and the DLF of the whole of the IEEE 69-bus system can be compared according to data presented in Table 5 and Table 6. In Table 5, as the worst-case with the more voltage difference, the minimum voltage of each case and its corresponding bus is chosen and compared with the voltage calculated of that bus while the DLF is performed on the whole of the grid. In Table 6, a common bus, which exists in all of the cases is chosen and the comparison of the voltage of that bus achieved using DLF of the whole grid and the DLF using ZAFDRC is presented. The convergence is achieved when the voltage error becomes less than 0.0001p.u.. Both tables show that the maximum voltage error

Table 4 Comparison of the DLF time of the IEEE 69-bus system plus the PC matrix building time in different cases.

Cases	DLF results of a part of the grid using the proposed method			
No DG	Solution time [ms]	551.8		
1 DG connected	Bus	61		
	Predefined reactive [kVAr] according to the scenario	1133.81		
	Calculated reactive [kVAr]	1283.30		
	Desired reactive to be calculated [kVAr]	1283.81		
	$V_{1\,spec}^{61}$ [p.u.]	0.9998		
	Calculated V_1^{61}	0.9998		
	Solution time [ms]	α = 7000	69.29	
		α = 1	117570	
2 DGs connected	Bus	61	17	
	Predefined reactive (kVAr) according to the scenario	1140.2	343.2	
	Calculated reactive (kVAr)	1254.2	378.1	
	Desired reactive to be calculated (kVAr)	1253.6	377.3	
	$V_{1\,spec}^{61,17}$ [p.u.]	1.0024	1.0012	
	Calculated $V_1^{61,17}$	1.0024	1.0012	
	Solution time [ms]	α = 7000	102.91	
		α = 1	202590	
3 DGs connected	Bus	61	17	50
	Predefined reactive [kVAr] according to the scenario	1097	330	439
	Calculated reactive [kVAr]	1189.4	351.86	471.87
	Desired reactive to be calculated [kVAr]	1186	356	474
	$V_{1\,spec}^{61,17,50}$ [p.u.]	0.99790	0.99890	0.99960
	Calculated $V_1^{61,17,50}$	0.99789	0.99889	0.99959
	Solution time [ms]	α =7000	208.20	
		α =1	276240	

Table 5 Comparison of the network voltages achieved using DLF of the whole grid and the DLF of grid while the ZAFDRC is used.

Cases	Minimum voltage of network calculated using ZAFDRC [p.u.]	Voltage of the bus achieved using ZAFDRC while the DLF of the whole grid is performed [p.u.]
1 DG connected	0.99329 @ 9	@ 9 → 0.99328
2 DGs connected	0.99550 @ 12	@ 12 → 0.99551
3 DGs connected	0.99410 @ 12	@ 12 → 0.99410

Table 6 Comparison of the voltage achieved using DLF of the whole grid and ZAFDRC DLF for a specified bus.

Cases	Voltage of bus 9 calculated using ZAFDRC [p.u.]	Voltage of bus 9 while the DLF of the whole of the grid is performed [p.u.]
1 DG connected	0.99329	0.99328
2 DGs connected	0.99731	0.99732
3 DGs connected	0.99632	0.99632

achieved using ZAFDRC is less than 0.0001p.u. (the convergence condition) and verifies the accuracy of the proposed method.

5.2 IEEE 123-Bus System

As an unbalanced and larger network with a heavier computational burden, the IEEE 123-bus system is considered here to validate the speed and accuracy of the proposed method for unbalanced distribution networks. The single line diagram of this network is shown in Fig. 7. Here, it is supposed that three DG units are located at buses 26, 44, 60 on the system and the load flow is calculated on the section shown in Fig. 7. The black path shown in Fig. 7 shows the case, that there are three DGs connected to the network. The grey path presents the lateral feeders and the dashed and dot-dashed paths show the cases that there are 1 and 2 DG(s) connected to the network. DGs are modeled as PV buses as declared in Section 2. In order to show the effect of α, the load flow in each case is calculated using $\alpha = 1$ and $\alpha = 4000$ (the proposed method). For a better comparison the same scenario, as declared for the IEEE 69-bus system, is considered here for the IEEE 123-bus system. The data of DGs and the buses that those are connected to are presented in Table 7.

Table 8 shows the DLF time results. Comparing the case with no DG unit with the other cases shows the really high speed of the proposed method. The voltage difference error results are presented in Tables 9 and 10. Like Tables 5 and 6 for the IEEE 69-Bus system, the data presented in Tables 9 and 10 validates the high accuracy of the proposed method in the IEEE 123-Bus system with the voltage difference error less than 0.0001p.u. As an interesting issue, comparing the solution time with $\alpha = 1$ of the corresponding cases having the same DG unit numbers in Tables 4 and 8 shows the more effect of the system size rather than the unbalancing of the system.

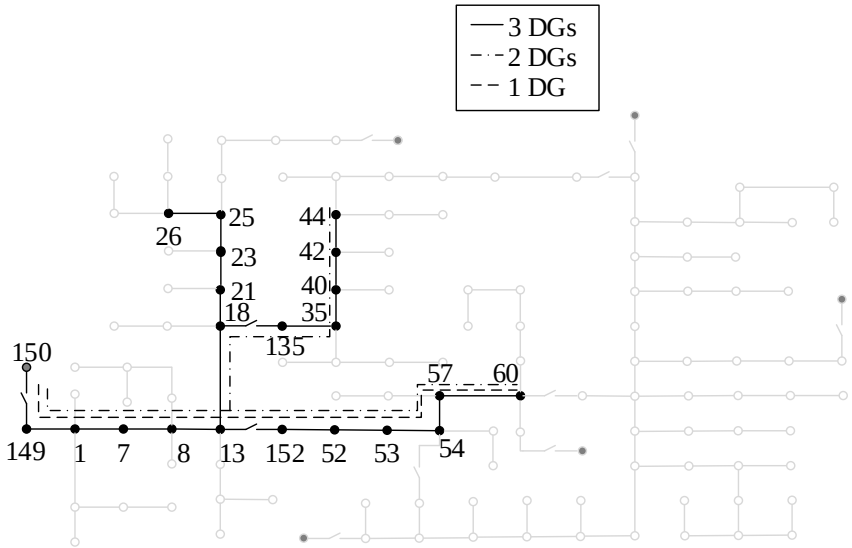

Fig. 7 Single line diagram of the IEEE 123-bus system and the path chosen for the DLF.

Table 7 Data of DGs connected to the IEEE 123-bus system.

Cases		Installed DG schedule		
1 DG connected	Bus	60		
	Size [kVA]	1100		
	P DG [kW]	800		
	Q DG [kVAr]	600		
	Voltage @ bus [p.u.]	0.96638		
2 DGs connected	Bus	60	44	
	Size [kVA]	1100	400	
	P DG [kW]	800	300	
	Q DG [kVAr]	600	145	
	Voltage @ bus [p.u.]	0.96971	0.96351	
3 DGs connected	Bus	60	26	44
	Size [kVA]	1100	200	400
	P DG [kW]	800	100	300
	Q DG [kVAr]	600	60	145
	Voltage @ bus [p.u.]	0.97087	0.96883	0.96525

It is known that in an unbalanced system the computational burden is 3 times more than the computational burden in a balanced system. Comparing the solution time of the case with one DG unit and $\alpha = 1$ in Tables 4 and 8 shows that although the 123-Bus system is an unbalanced system and the 69-Bus system is a balanced one, but the solution time in the 69-Bus system is very longer. This occurs due to the size of the system in this case, which shows the effectiveness of the zooming based approach. In the case with one DG unit, according to Figs. 6 and 7, only 18 buses of 69 buses of the grid nodes are included in DLF of the 69-Bus system, while the included buses in 123-Bus system DLF are 10 ones. The more interesting issue is actually that with a great compensation factor (that is tuned for a determined network) this time difference is almost completely eliminated which shows the high effectiveness of the compensation factor.

6 Conclusion

The present study was designed to determine the effect of the proposed method (ZAFDRC) in decreasing the DLF time of the active radial distribution networks. Two systems were considered in this paper. The IEEE 69-bus and the IEEE 123-bus systems were used to

Table 8 Comparison of the DLF time of the IEEE 123-bus system plus the PC matrix building time in different cases.

Cases	DLF results of a part of the grid using the proposed method			
No DG	Solution time [ms]	2135.9		
1 DG connected	Bus	60		
	Predefined kVAr	450		
	Calculated kVAr	601.4		
	Desired reactive to be calculated [kVAr]	600		
	$V_{1\,spec}^{60}$ [p.u.]	0.96638		
	Calculated V_1^{60}	0.96639		
	Solution time [ms]	$\alpha = 4000$	204.34	
		$\alpha = 1$	35456	
2 DGs connected	Bus	60	44	
	Predefined kVAr	490	105	
	Calculated kVAr	599.24	147.3	
	Desired reactive to be calculated [kVAr]	600	145	
	$V_{1\,spec}^{60,44}$ [p.u.]	0.96971	0.96351	
	Calculated $V_1^{60,44}$	0.96970	0.96354	
	Solution time [ms]	$\alpha = 4000$	157.68	
		$\alpha = 1$	58693	
3 DGs connected	Bus	60	26	44
	Predefined kVAr	502.95	42.35	109.7
	Calculated kVAr	600.167	60.182	144.85
	Desired reactive to be calculated [kVAr]	600	60	145
	$V_{1\,spec}^{60,44,26}$ [p.u.]	0.97087	0.96883	0.96525
	Calculated $V_1^{60,44,26}$	0.97089	0.96883	0.96525
	Solution time [ms]	$\alpha = 4000$	240.85	
		$\alpha = 1$	82961	

Table 9 Comparison of the network voltages achieved using DLF of whole grid and the DLF of grid while the ZAFDRC is used.

Cases	Minimum voltage of network calculated using ZAFDRC [p.u.]	Voltage of the bus achieved using ZAFDRC while the DLF of the whole grid is performed [p.u.]
1 DG connected	0.96639 @ 60	@ 60 → 0.96640
2 DGs connected	0.96354 @ 44	@ 44 → 0.96352
3 DGs connected	0.96525 @ 44	@ 44 → 0.96525

Table 10 Comparison of the voltage achieved using DLF of the whole grid and ZAFDRC DLF for a specified bus.

Cases	Voltage of bus 53 calculated using ZAFDRC [p.u.]	Voltage of bus 53 while the DLF of the whole of the grid is performed [p.u.]
1 DG connected	0.96886	0.96894
2 DGs connected	0. 97218	0. 97220
3 DGs connected	0. 97335	0. 97335

show the high performance of the proposed method to calculate the load flow of the balanced and unbalanced radial distribution networks. According to the simulation results, the high performance of the proposed method in decreasing the DLF time and keeping the load flow accuracy as high as possible at the presence of DGs operating in PV-mode was validated. In addition, a faster approach for building the PC matrix using the $\mathbf{Y}_{BUS}$ matrix was proposed which causes the computational burden to be decreased. Moreover, the proposed approach makes the network modeling more flexible in cases with more than one supplying bus.

References

[1] H. Lee Willis, and W. G.Scott, *Distributed power generation: planning and evaluation*. CRC Press, 2000.

[2] A. Cataliotti, V. Cosentino, D. Di Cara, P. Russotto, E. Telaretti, and G. Tinè, "An innovative measurement approach for load flow analysis in MV smart grids," *IEEE Transactions on Smart Grid*, Vol. 7, No. 2, pp. 889–896, 2016.

[3] E. Santacana, G. Rackliffe, L. Tang, and X. Feng, "Getting smart," *IEEE Power and Energy Magazine*, Vol. 8, No. 2, pp. 41–48, 2010.

[4] P. P. Barker and R. W. de Mello, "Determining the impact of distributed generation on power systems: Part 1- Radial distribution systems," in *IEEE Power Engineering Society Summer Meeting*, Seattle, WA, USA, Vol. 3, pp. 1645–1656, 2000.

[5] R. J. Ranjith Kumar and A. Jain, "Load flow methods in distribution systems with dispersed generations: A brief review," in *IEEE 1st Conference on Power, Dielectric and Energy Management at NERIST (ICPDEN)*, Itanagar, India, pp. 1–4, 2015.

[6] C. Wang, A. Bernstein, J. Y. Le Boudec, and M. Paolone, "Explicit conditions on existence and uniqueness of load-flow solutions in distribution networks,", *IEEE Transactions on Smart Grid*, Vol. 9, No. 2, pp. 953–962, 2018.

[7] J. Martinez and J. Mahseredjian, "Load flow calculations in distribution systems with distributed resources. A review," in *IEEE Power and Energy Society General Meeting*, Detroit, MI, USA, pp. 1–8, 2011.

[8] A. Vargas and M. Samper, "Real-time monitoring and economic dispatch of smart distribution grids: High performance algorithms for DMS applications," *IEEE Transactions on Smart Grid*, Vol. 3, No. 2, pp. 866–877, 2012.

[9] L. de Araujo, D. Penido, N. A. Do Amaral Filho, and T. A. P. Beneteli, "Sensitivity analysis of convergence characteristics in power flow methods for distribution systems," *International Journal of Electrical Power & Energy Systems*, Vol. 97, pp. 211–219, 2017.

[10] D. Bhujel, B. Adhikary, and A. Mishra, "A load flow algorithm for radial distribution system with distributed generation," in *IEEE Third International Conference on Sustainable Energy Technologies (ICSET)*, Kathmandu, Nepal, pp. 375–380, 2012.

[11] W. Tinney and C. Hart, "Power flow solution by newton's method," *IEEE Transactions on Power Apparatus and Systems*, Vol. 86, No. 11, pp. 1449–1460, 1967.

[12] W. H. Kersting and D. L. Mendive, "An application of ladder network theory to the solution of three phase radial load flow problem," in *IEEE Power Engineering Society Summer Meeting*, New York, Jan. 1976.

[13] M. M. M. Aman, G. B. Jasmon, A. H. Abu Bakar, H. Mokhlis, and K. Naidu, "Graph theory-based radial load flow analysis to solve the dynamic network reconfiguration problem," *International Transactions on Electrical Energy Systems*, Vol. 26, No. 4, pp. 783–808, 2015.

[14] A. Vural, "Interior point-based slack-bus free-power flow solution for balanced islanded microgrids," *International Transactions on Electrical Energy Systems*, Vol. 26, No. 5, pp. 968–992, 2015.

[15] N. Yang and H. Chen, "Three-phase power-flow solutions using decomposed quasi-Newton method for unbalanced radial distribution networks," *IET Generation, Transmission & Distribution*, Vol. 11, No. 14, pp. 3594–3600, 2017.

[16] K. Saxena and A. Abhyankar, "Agent-based decentralised load flow computation for smart management of distribution system," *IET Generation, Transmission & Distribution*, Vol. 11, No. 3, pp. 605–614, 2017.

[17] M. Abedini, "A novel algorithm for load flow analysis in island microgrids using an improved evolutionary algorithm," *International Transactions on Electrical Energy Systems*, Vol. 26, No. 12, pp. 2727–2743, 2016.

[18] V. Veerasamy, R. Ramachandran, M. Thirumeni, and B. Madasamy, "Load flow analysis using generalised Hopfield neural network," *IET Generation, Transmission & Distribution*, Vol. 12, No. 8, pp. 1765–1773, 2018.

[19] M. Shakarami, H. Beiranvand, A. Beiranvand, and E. Sharifipour, "A recursive power flow method for radial distribution networks: Analysis, solvability and convergence," *International Journal of Electrical Power & Energy Systems*, Vol. 86, pp. 71–80, 2017.

[20] U. Ghatak and V. Mukherjee, "A fast and efficient load flow technique for unbalanced distribution system," *International Journal of Electrical Power & Energy Systems*, Vol. 84, pp. 99–110, 2017.

[21] R. Berg, E. Hawkins, and W. Pleines, "Mechanized calculation of unbalanced load flow on radial distribution circuits," *IEEE Transactions on Power Apparatus and Systems*, Vol. 86, No. 4, pp. 415–421, 1967.

[22] D. I. H. Sun, S. Abe, R. R. Shoults, M. S. Chen, P. A. E. P. Eichenberger, and D. Farris, "Calculation of energy losses in a distribution system," *IEEE Transactions on Power Apparatus and Systems*, Vol. 99, No. 4, pp. 1347–1356, 1980.

[23] G. W. Stagg and A. H. El-Abiad, *Computer methods in power system analysis*. McGraw-Hill, New York, 1968.

[24] P. S. Nagendra Rao and K. S. Prakasa Rao, "A fast load flow method for radial distribution systems," in *Proceeding of Platinum Jublee Conferance on Systems and Signal Processing*, IISc Bangalore, pp. 71–474, 1986.

[25] Y. Zhu and K. Tomsovic, "Adaptive power flow method for distribution systems with dispersed generation", *IEEE Transactions on Power Delivery*, Vol. 17, No. 3, pp. 822–827, 2002.

[26] J. H. Teng, "A direct approach for distribution system load flow solutions," *IEEE Transactions on Power Delivery*, Vol. 18, No. 3, pp. 882–887, 2003.

[27] M. AlHajri and M. El-Hawary, "Exploiting the radial distribution structure in developing a fast and flexible radial power flow for unbalanced three-phase networks," *IEEE Transactions on Power Delivery*, Vol. 25, No.1, pp. 378–389, 2010.

[28] A. Eltantawy and M. Salama, "A novel zooming algorithm for distribution load flow analysis for smart grid," *IEEE Transactions on Smart Grid*, Vol. 5, No. 4, pp. 1704–1711, 2014.

[29] L. Gallego, E. Carreno, and A. Padilha-Feltrin, "Distributed generation modelling for unbalanced three-phase power flow calculations in smart grids," in *IEEE IEEE/PES Transmission and Distribution Conference and Exposition: Latin America (T&D-LA)*, pp. 323–328, 2010.

[30] S. Khushalani, J. Solanki, and N. Schulz, "Development of three-phase unbalanced power flow using PV and PQ models for distributed generation and study of the impact of DG models," *IEEE Transactions on Power Systems*, Vol. 22, No. 3, pp. 1019–1025, 2007.

[31] D. Hung and N. Mithulananthan, "Multiple distributed generator placement in primary distribution networks for loss reduction," *IEEE Transactions on Industrial Electronics*, Vol. 60, No. 4, pp. 1700–1708, 2013.

O. Honarfar was born in Iran in 1991. Now he is pursuing the Ph.D. degree in Electric Power Engineering at the University of Kashan, Kashan, Iran. His areas of interest include smart grid, distribution systems, and power electronics.

A. Karimi was born in Iran in 1984. He is an Assistant Professor at the University of Kashan, Kashan, Iran. He received the B.Sc. degree from the University of Kashan in 2007, the M.Sc. degree from the University of Tehran, Tehran, Iran in 2009, and the Ph.D. degrees from Tarbiat Modares University (TMU), Tehran, Iran, in 2014, all in Electric Power Engineering. He worked for Iranian Power System Engineering Research Center (IPSERC), as a researcher, during 2009–2015. His main research interests are power system operation, electricity market, electric distribution systems, and smart grids.